

Reversible Luminescence Modulation upon Electric Field on a Full Solid-State Device Based on Lanthanide Dimers

Xiaohui Yi, Jie Shang, Liang Pan, Hongwei Tan, Bin Chen, Gang Liu, Gang Huang, Kevin Bernot, Olivier Guillou, and Run-Wei Li

ACS Appl. Mater. Interfaces, **Just Accepted Manuscript** • DOI: 10.1021/acsami.6b04451 • Publication Date (Web): 31 May 2016

Downloaded from <http://pubs.acs.org> on June 1, 2016

Just Accepted

“Just Accepted” manuscripts have been peer-reviewed and accepted for publication. They are posted online prior to technical editing, formatting for publication and author proofing. The American Chemical Society provides “Just Accepted” as a free service to the research community to expedite the dissemination of scientific material as soon as possible after acceptance. “Just Accepted” manuscripts appear in full in PDF format accompanied by an HTML abstract. “Just Accepted” manuscripts have been fully peer reviewed, but should not be considered the official version of record. They are accessible to all readers and citable by the Digital Object Identifier (DOI®). “Just Accepted” is an optional service offered to authors. Therefore, the “Just Accepted” Web site may not include all articles that will be published in the journal. After a manuscript is technically edited and formatted, it will be removed from the “Just Accepted” Web site and published as an ASAP article. Note that technical editing may introduce minor changes to the manuscript text and/or graphics which could affect content, and all legal disclaimers and ethical guidelines that apply to the journal pertain. ACS cannot be held responsible for errors or consequences arising from the use of information contained in these “Just Accepted” manuscripts.

Reversible Luminescence Modulation upon Electric Field on a Full Solid-State Device Based on Lanthanide Dimers

Xiaohui Yi^{a,b}, Jie Shang^{a,b}, Liang Pan^{a,b}, Hongwei Tan^{a,b}, Bin Chen^{a,b}, Gang Liu^{a,b*}, Gang Huang^c, Kevin Bernot^{c*}, Olivier Guillou^c, Run-Wei Li^{a,b*}

^aKey Laboratory of Magnetic Materials and Devices, Ningbo Institute of Materials Technology and Engineering, Chinese Academy of Sciences, Ningbo, 315201, P. R. China.

^bZhejiang Province Key Laboratory of Magnetic Materials and Application Technology, Ningbo Institute of Materials Technology and Engineering, Chinese Academy of Sciences, Ningbo, 315201, P. R. China.

^cInstitut des Sciences Chimiques de Rennes, UMR 6226 INSA-Rennes, 20 avenue des buttes de Coësmes, 35708 Rennes, France.

*To whom all correspondence should be addressed: liug@nimte.ac.cn (Prof. Dr. G. Liu), runweili@nimte.ac.cn (Prof. Dr. R.-W. Li), kevin.bernot@insa-rennes.fr (Prof. Dr. K. Bernot)

1
2
3
4
5
6
7 **Abstract:** Switching luminescence of lanthanide-based molecules through external electric field
8
9 is considered as a promising approach toward novel functional molecule-based devices. Classic
10 routes use casted films and liquid electrolyte as media for redox reactions. Such protocol, even if
11 efficient, is relatively hard to turn into an effective solid-state device. In this work, we explicitly
12 synthesize lanthanide-based dimers whose luminescent behaviour is affected by the presence of
13 Cu^{2+} ions. Excellent evaporability of the dimers and utilisation of Cu^{2+} -based solid-state
14 electrolyte makes it possible to reproduce solution behaviour at the solid-state. Reversible
15 modulation of Cu^{2+} ions transport can be achieved by an electric field in a solid-state device,
16 where lanthanide-related luminescence is driven by electric field. These findings provide a
17 proof-of-concept alternative approach for electrically-driven modulation of solid-state
18 luminescence and show promising potential for information storage media in the future.
19
20
21
22
23
24
25
26
27
28
29
30
31
32

33 **Keywords:** Luminescence modulation • Lanthanide ions • Ion transport • All-solid state •
34
35 Electrical driven
36
37
38
39
40
41
42
43
44
45
46
47
48
49
50
51
52
53
54
55
56
57
58
59
60

Introduction

Non-volatile manipulation of luminescence through external stimuli is considered as a fascinating and promising approach for applications such as memories, displays and sensors.¹⁻⁵ In particular, the modulation of luminescence with electric field as external stimuli carries unique advantages for information storage. For instance, as the stored information can be optically and remotely readout with fast transmission rate and anti-interference characteristics,⁶ high density recording can be achieved by properly designing the structure of electronic memories.⁷⁻⁸ The realization of such optoelectronic circuits requires smart luminescent molecules or materials, in which not only reversible switching of luminescence is necessary when being subjected to external electric field, but also various luminescence colors should be obtained in order to provide crosstalk-free readout among different storing units. Lanthanide-based complexes are ideal candidates for the construction of such systems because of their multi-color, narrow-bandwidth and long-lived luminescence properties.⁹ Nevertheless, the tedious film deposition procedure and the requisition of liquid supporting electrolyte for redox reactions upon electric field still impede them from direct application.¹⁰⁻¹²

In this work, we propose and demonstrate a proof-of-concept strategy that combines two interesting findings for the effective modulation of luminescence of lanthanide-based complexes in solid state: i) the luminescence of lanthanide compounds containing Lewis basic pyridyl sites can be efficiently quenched by Cu^{2+} ions.^{13,14} ii) Cu^{2+} ions can be transported and controllably redistributed by electrical field in solid-state media.¹⁵⁻¹⁷ Based on the above considerations, we have synthesized a new series of lanthanide-based dinuclear complexes **LnPraNO**, of formula $[\text{Ln}(\text{hfac})_3(\text{PraNO})]_2$ (where Ln= Eu, Tb, Dy, hfac= hexafluoroacetylacetonate, PraNO = pyrazine-N-oxide). These complexes are evolutions of **LnPyNO** dimers of formula

1
2
3
4
5
6 [Ln(hfac)₃(PyNO)]₂ (PyNO = pyridine-N-oxide) that are strongly emissive and evaporable and
7
8 that some of us previously reported.¹⁸ In **LnPraNO** the aromatic ligand that bridge the
9
10 lanthanides possesses an uncoordinated Lewis basic pyridyl site that makes the luminescence of
11
12 these compounds highly sensitive to the presence of Cu²⁺ ions in solution. Furthermore, an
13
14 ITO/**LnPraNO**/Cu²⁺ ions@PEO/Pt (ITO = Indium Tin Oxides, PEO = polyethylene oxide)
15
16 structured solid-state devices based on these dimers can be designed and we demonstrate that the
17
18 reversible modulation of lanthanide-related luminescence behavior upon electric field is possible
19
20 through electric field-induced transport of Cu²⁺ ions across the dimer-based and electrolyte
21
22 layers.
23
24
25
26
27

28 **Results and Discussion**

29
30 Single-crystals of the Dy derivative (**DyPraNO**) have been obtained and main structural data are
31
32 reported in Table S1. Isostructurality of **EuPraNO**, **TbPraNO** and **DyPraNO** is verified on the
33
34 basis of comparison of their X-ray diffraction powder patterns (**Figure S1**). **DyPraNO**
35
36 crystallizes in the C2/c space group (N°15) (**Figure 1**) and is similar to the previously reported
37
38 dimer.¹⁸ The molecule is made of two Dy(hfac)₃ moieties connected by two pyrazine N-oxide
39
40 ligands. The Dy³⁺ ions are in a distorted square antiprism coordination environment close to a
41
42 D4d site symmetry (**Figure S2**). The intramolecular Dy-Dy distance is 4.10(6) Å. Each dimer is
43
44 well isolated with shortest interdimer Dy-Dy distance of 9.12 (1) Å.
45
46
47
48
49

50 The emissive properties of all the derivatives have been investigated in the solid
51
52 polycrystalline state at room temperature. As shown in **Figure 2a**, all compounds exhibit
53
54 characteristic luminescence of lanthanide ions when excited at 350 nm. The **EuPraNO**
55
56 derivatives exhibit the characteristic emission that corresponds to ⁵D₀ → ⁴F_J (J = 0 - 4) transitions.
57
58
59
60

1
2
3
4
5
6 For the **TbPraNO** and **DyPraNO**, well defined peaks are observed because of $^5D_4 \rightarrow ^4F_J$ ($J = 0 -$
7
8
9 6) and $^4F_{9/2} \rightarrow ^6H_J$ ($J = 11/2 - 15/2$) transitions, respectively. The excitation spectra of these
10
11 compounds are reported in **Figure S3**. The quantum yields are 14.1%, 17.2% and 0.1%,
12
13 respectively.
14
15

16
17 Generally, the luminescence of lanthanide complexes is arising from the 4f electron
18
19 transition from the excited states to the ground state, and may be enhanced through antenna
20
21 effect. For instance, the presence of organic ligand will lead to increased absorbance of UV light,
22
23 while the subsequent energy transfer from the ligands into the excited 4f state of the lanthanide
24
25 ions will intensify the luminescent intensity of the material. On the other hand, the uncoordinated
26
27 nitrogen atoms of the pyrazine N-oxide ligand are expected to be good coordination sites for 3d
28
29 ions such as Cu^{2+} . The interaction between the Cu^{2+} ions and the pyridyl N atoms will introduce
30
31 the additional non-radiative electron exchange pathways, which may reduce the antenna
32
33 efficiency of the organic ligand around lanthanide ions and quench the luminescence of the
34
35 lanthanide complexes.¹⁴ Quenching effect of Cu^{2+} has been first investigated on ethanoic
36
37 solutions of the **LnPraNO** series and clear diminution of the luminescence intensity is observed
38
39 upon addition of copper nitrate solution. Remarkably, equimolar copper-based solutions led to a
40
41 100 times reduction of the luminescence intensity on **EuPraNO** (**Figure 2b**). When similar
42
43 experiment is performed on the $[Eu(hfac)_3(PyNO)]_2$ dimer,¹⁸ the compound without
44
45 uncoordinated N atoms, only 50% decreasing of intensity is observed (**Figure S4**). This may
46
47 suggest a possible Cu^{2+} coordination on the uncoordinated N atom of the pyrazine ligand. For the
48
49 other derivatives of **TbPraNO** and **DyPraNO**, a decrease of 80% and 75% of the luminescence
50
51 intensity is observed respectively.
52
53
54
55
56
57
58
59
60

1
2
3
4
5
6 This quenching effect can be rationalized by a modified Stern-Volmer equation that describes
7 the static and dynamic process during the quenching (1):
8

$$\ln(I_0/I) = \ln(1 + K_{SV}[M]) + V[M] \quad (1)$$

9
10
11
12 where I_0 and I are the luminescence intensities before and after addition of the copper nitrate
13 solution, $[M]$ is the stoichiometric ratio between the metal ion and **LnPraNO**, K_{SV} and V are the
14 dynamic and static quenching effect coefficients of the metal ion, respectively.¹⁹ The V value is
15 estimated to be 3.56, 1.78 and 1.24, for **EuPraNO**, **TbPraNO** and **DyPraNO** respectively, while
16 the K_{SV} value that describe the collisional process is smaller than 0.1 (**Table S2** and **Figure S5**).
17
18
19
20
21
22
23
24

25
26 The above findings in liquid samples provide fundamental supporting for the proposed target
27 of modulating lanthanide compound luminescence in solid state. The good volatility and
28 robustness of **LnPraNO** make possible the design of a solid-state multilayer structure (**Figure**
29 **3a**, **3b** and **Figure S6**). Here, $\text{Cu}(\text{NO}_3)_2/\text{PEO}$ layer has been selected as the copper ions
30 providing layer since Cu^{2+} ions containing PEO is one of the typical solid-state electrolytes.²⁰
31 ITO electrodes with good electrical conductivity and excellent optical transparency were
32 fabricated as top electrode.²¹ As illustrated in **Figure 3c**, when an external negative electric field
33 is applied onto the ITO/**LnPraNO**/ $\text{Cu}(\text{NO}_3)_2@\text{PEO}/\text{Pt}$ device, the Cu^{2+} ions are expected to be
34 injected into the **LnPraNO** layers and to provoke the quenching of the luminescence of the
35 **LnPraNO** complexes (**State I**). When a positive electrical-field is applied, the Cu^{2+} ions are
36 expected to be pumped back into the PEO hosting layer and the luminescence of **LnPraNO**
37 complexes shall be recovered (**State II**).
38
39
40
41
42
43
44
45
46
47
48
49
50
51
52

53
54 Experimental data agreed well with the above model and the evolution of luminescence
55 intensity upon electric field variation for the Eu-based device is depicted in **Figure 4**. A negative
56 voltage is applied for 5 seconds to the device in order to induce Cu^{2+} migration where the
57
58
59
60

1
2
3
4
5
6 photoluminescence spectra are recorded after removing the electric field. The photoluminescence
7
8 (PL) intensity changes is observed for a minimum bias voltage of -1.5 V while for -2.5 V a 60%
9
10 decrease of the higher emission peak (615 nm) of **EuPraNO** is achieved (**Figure 4a**). When a
11
12 bias voltage of 3V is applied for 5 seconds and removed, the PL intensity could be recovered,
13
14 suggesting that the luminescence modulation operation of the device is fully reversible and the
15
16 compound was not destroyed. More importantly, the luminescent intensity remains stable when
17
18 the applied electric field is switched off (e. g., after 60 s as shown in **Figure 4b**), indicating that
19
20 non-volatile modulation of the device luminescence has been achieved by the present strategy.
21
22 By defining the highly luminescent state (**Initial state** and **State II**) as the ON state and the low
23
24 luminescence state (**State I**) as the OFF state, repeatable ON/OFF switching behavior can be
25
26 obtained in the lanthanide compounds-based molecular devices (**Figure 4c**).
27
28
29
30
31

32
33 It is noteworthy that luminescence change in these devices is not due to any redox reaction
34
35 that involves the lanthanide ion. In fact, such reaction is very unlikely to occur because i)
36
37 previous studies on the electrochemical properties of lanthanide-based β -diketonate complexes
38
39 demonstrate their difficult reduction in standard conditions;²² ii) reversibility would not be
40
41 observable as reduction may induce the de-coordination of the organic ligand and the lanthanide
42
43 and so annihilation of the antenna effect that promote lanthanide luminescence in the device; iii)
44
45 solution behavior upon variable Cu^{2+} concentration (**Figure 2**) match well with the observed
46
47 solid-state behavior. Consequently we can assume that the luminescent intensity change is
48
49 induced by the transport and redistribution of Cu^{2+} ions by the electric field in the **LnPraNO**
50
51 layer. This argument is verified by the dynamic process of the electrical field-induced PL change
52
53 (**Figure 4b** and **Figure S7**). After being stimulated with voltage pulse of -2.5 V, PL intensity at
54
55 615 nm drops at 53% of its nominal value and then relaxes around 60% of the original PL
56
57
58
59
60

1
2
3
4
5
6 intensity. This phenomenon is quite similar to the resistance relaxation induced by a ionic
7
8 transport discussed in several previous works.²³ The content of the ion Cu^{2+} ions injected upon -
9
10 2.5 V was estimated to be 0.20 molar fraction of **EuPraNO** molecules in the luminescent layer
11
12 according to equation (1). This is in agreement with the behavior observed in solution.
13
14

15
16 To further confirm the efficiency of the pyrazine ligand toward Cu^{2+} coordination, a device
17
18 based on the pyridine-based dimers previously mentioned (**EuPyNO**) is constructed and exposed
19
20 to the very similar operating conditions.¹⁸ It shows a lower quenching effect (80% instead of
21
22 60% of the nominal intensity is conserved) (**Figure S8**). This may support the hypothesis of a
23
24 strong interaction of the Cu^{2+} ions with the uncoordinated N atoms in the pyrazine-based
25
26 emissive layer as targeted in this study.
27
28
29
30

31
32 The devices based on Tb and Dy derivatives as luminescent layer exhibit similar but less
33
34 spectacular voltage-induced luminescence modulation behaviors. For -2.5 V voltage, the
35
36 luminescent intensities of the Tb and Dy-based devices are quenched about 65% and 70%
37
38 respectively, as shown in **Figure 5a** and **5b**. The Cu^{2+} ions injected are estimated to be 0.21 and
39
40 0.26 mole fraction of the **LnPraNO** molecules in the layers according to equation (1), for Tb and
41
42 Dy-based device, respectively. These values are once again in agreement with what observed in
43
44 solution together with the less efficient quenching effect compared with the Eu-based device.
45
46 Similar to ITO/**EuPraNO**/ $\text{Cu}(\text{NO}_3)_2$ @PEO/Pt unit, the photoluminescence of each measured Dy
47
48 and Tb-based unit could be recovered when a positive potential was set at 3 V for 5 seconds. The
49
50 luminescent switching is reversible as well (**Figure 5c** and **5d**). The modulation of the Eu^{3+} , Tb^{3+}
51
52 and Dy^{3+} -related luminescence with their distinguishable colors of red, green and yellow
53
54 respectively by the electric field present herein (**Figure 6**) will allow these structures to be used
55
56 as individual storage units in electro-optical device according their wavelength and intensity.
57
58
59
60

1
2
3
4
5
6
7
8
9
10
11
12
13
14
15
16
17
18
19
20
21
22
23
24
25
26
27
28
29
30
31
32
33
34
35
36
37
38
39
40
41
42
43
44
45
46
47
48
49
50
51
52
53
54
55
56
57
58
59
60

Moreover, lanthanide ions have also attracted considerable attention for molecular magnetic information storage since their huge magnetic anisotropy permitted the observation of single-molecule magnetic (SMM) behavior.^{24,25} In **DyPraNO** compounds, typical slow single-molecule magnetic relaxation with an effective energy barrier of 176.6 K was observed (**Figure S9** and **S10**). Consequently ITO/**DyPraNO**/Cu(NO₃)₂@PEO/Pt maybe key to investigate the possibility of combined magnetic and optical information storage devices in the future.

Conclusion

In summary, a series of evaporable β -diketonate Ln-based dimers (**LnPraNO**) has been synthesized. Tb, Dy and Eu derivatives exhibit luminescence upon UV irradiation that is drastically modified upon Cu²⁺ ions addition in ethanol solution. The construction of a complete solid state ITO/**LnPraNO**/Cu ions@PEO/Pt device (Ln = Eu, Tb, and Dy) make possible that these properties can be transferred at the solid state. In other words, we report a proof-of-concept full solid-state optoelectronic information storage unit, wherein one can write the data with an electrical stimulus, while read through the photoluminescence output signals according to their wavelength and intensities. Additional bistability of slow single-molecule magnetic relaxation of the **DyPraNO** compounds may also provide more flexible read/write approach to increase the information storage abilities of such systems in the future.

Experimental section

Synthetic Procedure. All reagents were analytical grade and used as received. Ln(hfac)₃·2H₂O precursors were synthesized accordingly to previously reported methods.²⁶ Pyrazine N-oxide was purchased from TCI chemicals. Ln(hfac)₃·2H₂O (0.2 mmol) (Ln= Dy, Eu) is added to 15mL boiling CHCl₃. Then a 10ml dry CHCl₃ solution of Pyrazine N-oxide (0.2 mmol) was added drop by drop. The resulting boiling mixture was stirred for 5 min, then cooled to room temperature. After some days of slow evaporation, big pale yellow (Tb³⁺, Dy³⁺, Eu³⁺) prisms are obtained. Elemental analysis calcd. (%) for F₃₆C₃₈H₁₄Dy₂N₄O₁₄: C: 25.94, H: 0.80, N: 3.18; Found: C: 26.13, H: 0.85, N: 3.21. calcd. (%) for F₃₆C₃₈H₁₄Eu₂N₄O₁₄: C: 26.23, H: 0.81, N: 3.22; Found: C: 26.32, H: 0.84, N: 3.22. calcd. (%) for F₃₆C₃₈H₁₄Eu₂N₄O₁₄: C: 26.02, H: 0.80, N: 3.19; Found: C: 26.24, H: 0.84, N: 3.21.

Crystal structure determination. Single crystal was mounted on a APEXII AXS-Bruker diffractometer equipped with a CCD camera and a graphite-monochromated MoK radiation source (d=0.71073 Å), from the Centre de Diffraction (CDFIX), Université de Rennes 1, France. Data were collected at 150K. Structure was solved with a direct method using the SIR-97 program²⁷ and refined with a full-matrix least-squares method on F² using the SHELXL-97 program²⁸ and WinGx interface.²⁹ Crystallographic data are summarized in Table S1. CCDC-1455178 contains the supplementary crystallographic data for this paper. These data can be obtained free of charge from The Cambridge Crystallographic Data Centre via www.ccdc.cam.ac.uk/data_request/cif.

Powder X-ray diffraction. Diagrams have been collected using a Panalytical X'Pert Pro diffractometer with an X'Celerator detector. The typical recording conditions were 45kV, 40mA for Cu-Kα (λ=1.542Å), the diagrams were recorded in θ-θ mode in 6 min between 5° and 45° (8378 measurements).

Luminescence Measurements. Powder state and liquid state luminescent measurements were collected using Horiba-JobinYvon Fluorolog III spectrofluorometer. Spectrofluorometer was beforehand calibrated using the 467 nm most intense peak of the lamp for excitation wavelength and Raman emission peak of water at 397 nm for 350 nm UV irradiation. Luminescence spectra were all recorded at room temperature in identical operating conditions without turning the lamp

1
2
3
4
5
6 off to ensure a valid comparison between the emission spectra. Reproducibility of the
7 measurements has been carefully checked. All spectra have been recorded at λ_{exc} that is found to
8 be the maximum of the respective excitation spectra. Quantum yield measurement were
9 performed at 293 K by evaluating the ratio of emitted photons by absorbed photons, that is

$$10 \quad Q_y = (E_c - E_a) / (L_a - L_c) \quad (2)$$

11 where E_c is the integral of the emission spectrum of the sample, E_a is the integral of the emission
12 spectrum of the empty sphere, L_a is the integral of the blank absorption spectrum of the empty
13 sphere and L_c is the integral of the absorption spectrum of the sample.
14
15
16
17
18
19

20 **Device Fabrication.** The $\text{Cu}(\text{NO}_3)_2@\text{PEO}$ thin film was deposited on a commercially available
21 Pt/SiO₂/Si substrate with spin coating method. The **LnPraNO** thin film was then deposited on
22 the $\text{Cu}(\text{NO}_3)_2@\text{PEO}$ thin film by thermal deposition. After that, the transparent conductive ITO
23 thin film was then deposited on the previously mentioned thin films by using the pulsed laser
24 deposition system at room temperature with the oxygen pressure varied between 0.8 and 1 Pa.
25 The deposition frequency of ITO thin films was set to 1 Hz.
26
27
28
29
30
31

32 **Device structure characterization.** The crystalline structure of the as-deposited **LnPraNO**
33 films was investigated by grazing-incidence X-ray diffraction technique (GIXRD, Bruker AXS,
34 D8 Discover) using Cu-K α radiation. The incidence angle of X-ray beam was fixed at 1° and the
35 measurements were recorded with a step of 0.05° in the range of 5° to 45°. The thickness of the
36 films was determined using field-emission scanning electron microscopy (FESEM, Hitachi, S-
37 4800) with 10 kV accelerating voltage.
38
39
40
41
42

43 The photoluminescent intensities of ITO/ **LnPraNO** / $\text{Cu}(\text{NO}_3)_2\text{PEO}$ /Pt structures after applying
44 various electrical fields were measured on homemade probe station equipped with a precision
45 semiconductor parameter analyzer (Agilent B1500) and laser confocal luminescent microscopy
46 with Andor iR303 spectrometer. Importantly, the luminescence measurements were performed
47 after removing the applied electrical field in order to avoid possible electroluminescence.
48
49
50
51

52 **Magnetic dc and ac Measurements.** Samples were measured on polycrystalline state
53 compressed tightly by Polyethylene film to avoid in-field orientation of the crystallites.
54 Measurements were corrected for the diamagnetic contribution, as calculated with Pascal's
55
56
57
58
59
60

1
2
3
4
5
6 constants, and for the diamagnetism of the sample holder, as independently determined. Ac
7
8 susceptibility has been measured with Quantum Design MPMS magnetometer in the low
9
10 frequency range and PPMS magnetometer in the high frequency range.
11
12
13
14
15
16
17
18
19
20
21
22
23
24
25
26
27
28
29
30
31
32
33
34
35
36
37
38
39
40
41
42
43
44
45
46
47
48
49
50
51
52
53
54
55
56
57
58
59
60

Supporting Information

Additional structural, spectroscopic and magnetic properties of the lanthanide complexes. This material is available free of charge via the Internet at <http://pubs.acs.org>.

Corresponding Author

Prof. Dr. Gang Liu: liug@nimte.ac.cn,

Dr. Kevin Bernot: kevin.bernot@insa-rennes.fr,

Prof. Dr. Run-Wei Li: runweili@nimte.ac.cn.

Notes

The authors declare no competing financial interests.

Acknowledgement

We thank Dr. Pravarthana Dhanapal, Ms. Wuhong Xue and Mr. Xipao Chen for the discussion. This work was supported by the State Key Project of Fundamental Research of China (973 Program, 2012CB933004), National Natural Science Foundation of China (61504154, 11274322, 51303194, 61328402, 61306152, 11474295, 61574146, 51525103), China Postdoctoral Science Foundation Funded Project (2014M560499), the Instrument Developing Project of the Chinese Academy of Sciences (YZ201327), the Youth Innovation Promotion Association of the Chinese Academy of Sciences, Ningbo Major Project for Science and Technology (2014B11011), Ningbo Science and Technology Innovation Team (2015B11001), Ningbo Natural Science Foundation (2014A610152), and Ningbo International Cooperation Projects (2014D10005).

References

1. Zimmermann, S.; Wixforth, A.; Kotthaus, J. P.; Wegscheider, W.; Bichler, M., A Semiconductor-based Photonic Memory Cell. *Science* **1999**, 283 (5406), 1292-1295.
2. Mutai, T.; Satou, H.; Araki, K., Reproducible On-Off Switching of Solid-State Luminescence by Controlling Molecular Packing Through Heat-Mode Interconversion. *Nat. Mater.* **2005**, 4 (9), 685-687.
3. Sagara, Y.; Kato, T., Mechanically Induced Luminescence Changes in Molecular Assemblies. *Nat Chem* **2009**, 1 (8), 605-610.
4. Audebert, P.; Miomandre, F., Electrofluorochromism: from Molecular Systems to Set-Up and Display. *Chem. Sci.* **2013**, 4 (2), 575-584.
5. Sun, H.; Liu, S.; Lin, W.; Zhang, K. Y.; Lv, W.; Huang, X.; Huo, F.; Yang, H.; Jenkins, G.; Zhao, Q.; Huang, W., Smart Responsive Phosphorescent Materials for Data Recording and Security Protection. *Nat. Commun.* **2014**, 5, 3601-3609.
6. Ríos, C.; Stegmaier, M.; Hosseini, P.; Wang, D.; Scherer, T.; Wright, C. D.; Bhaskaran, H.; Pernice, W. H. P., Integrated All-photonic Non-volatile Multi-level Memory. *Nat. Photonics* **2015**, 9 (11), 725-732.
7. Kim, K.-H.; Gaba, S.; Wheeler, D.; Cruz-Albrecht, J. M.; Hussain, T.; Srinivasa, N.; Lu, W., A Functional Hybrid Memristor Crossbar-Array/CMOS System for Data Storage and Neuromorphic Applications. *Nano Lett.* **2012**, 12 (1), 389-395.
8. Zijlstra, P.; Chon, J. W. M.; Gu, M., Five-Dimensional Optical Recording Mediated by Surface Plasmons in Gold Nanorods. *Nature* **2009**, 459 (7245), 410-413.
9. Bünzli, J.-C.; Eliseeva, S., Basics of Lanthanide Photophysics. In *Lanthanide Luminescence*, Hänninen, P.; Härmä, H., Eds. Springer Berlin Heidelberg: 2011; Vol. 7, 1-45.
10. Di Piazza, E.; Norel, L.; Costuas, K.; Bourdolle, A.; Maury, O.; Rigaut, S., d-f Heterobimetallic Association between Ytterbium and Ruthenium Carbon-Rich Complexes: Redox Commutation of Near-IR Luminescence. *J. Am. Chem. Soc.* **2011**, 133 (16), 6174-6176.
11. Sato, T.; Higuchi, M., An Alternately Introduced Heterometallo-Supramolecular Polymer: Synthesis and Solid-state Emission Switching by Electrochemical Redox. *Chem. Commun.* **2013**, 49 (46), 5256-5258.
12. Tropiano, M.; Kilah, N. L.; Morten, M.; Rahman, H.; Davis, J. J.; Beer, P. D.; Faulkner, S., Reversible Luminescence Switching of A Redox-Active Ferrocene-Europium Dyad. *J. Am. Chem. Soc.* **2011**, 133 (31), 11847-11849.
13. Tang, Q.; Liu, S.; Liu, Y.; Miao, J.; Li, S.; Zhang, L.; Shi, Z.; Zheng, Z., Cation Sensing by A Luminescent Metal-Organic Framework with Multiple Lewis Basic Sites. *Inorg. Chem.* **2013**, 52 (6), 2799-2801.
14. Chen, B.; Wang, L.; Xiao, Y.; Fronczek, F. R.; Xue, M.; Cui, Y.; Qian, G., A Luminescent Metal-Organic Framework with Lewis Basic Pyridyl Sites for the Sensing of Metal Ions. *Angew. Chem. Int. Ed.* **2009**, 48 (3), 500-503.
15. Hu, B.; Zhu, X.; Chen, X.; Pan, L.; Peng, S.; Wu, Y.; Shang, J.; Liu, G.; Yan, Q.; Li, R.-W., A Multilevel Memory Based on Proton-Doped Polyazomethine with An Excellent Uniformity in Resistive Switching. *J. Am. Chem. Soc.* **2012**, 134 (42), 17408-17411.
16. Zhu, X.-J.; Shang, J.; Li, R.-W., Resistive Switching Effects in Oxide Sandwiched Structures. *Front. Mater. Sci.* **2012**, 6 (3), 183-206.

17. Zhu, X.; Su, W.; Liu, Y.; Hu, B.; Pan, L.; Lu, W.; Zhang, J.; Li, R.-W., Observation of Conductance Quantization in Oxide-Based Resistive Switching Memory. *Adv. Mater.* **2012**, *24* (29), 3941-3946.
18. Yi, X.; Bernot, K.; Pointillart, F.; Poneti, G.; Calvez, G.; Daiguebonne, C.; Guillou, O.; Sessoli, R., A Luminescent and Sublimable Dy-III-Based Single-Molecule Magnet. *Chem. - Eur. J.* **2012**, *18* (36), 11379-11387.
19. Melavanki, R. M.; Kusanur, R. A.; Kulakarni, M. V.; Kadadevarmath, J. S., Role of Solvent Polarity on the Fluorescence Quenching of Newly Synthesized 7,8-benzo-4-azidomethyl Coumarin by Aniline in Benzene-acetonitrile Mixtures. *J. Lumines.* **2008**, *128* (4), 573-577.
20. Lewandowski, A.; Stępnia, I.; Grzybowski, W., Copper Transport Properties in Polymer Electrolytes Based on Poly(ethylene oxide) and Poly(acrylonitrile). *Solid State Ionics* **2001**, *143* (3-4), 425-432.
21. Shang, J.; Liu, G.; Yang, H.; Zhu, X.; Chen, X.; Tan, H.; Hu, B.; Pan, L.; Xue, W.; Li, R.-W., Thermally Stable Transparent Resistive Random Access Memory based on All-Oxide Heterostructures. *Adv. Funct. Mater.* **2014**, *24* (15), 2171-2179.
22. Binnemans, K., Chapter 225 - Rare-earth beta-diketonates. In *Handbook on the Physics and Chemistry of Rare Earths*, Karl A. Gschneidner, J.-C. G. B.; Vitalij, K. P., Eds. Elsevier: 2005; Vol. Volume 35, 107-272.
23. Du, C.; Ma, W.; Chang, T.; Sheridan, P.; Lu, W. D., Biorealistic Implementation of Synaptic Functions with Oxide Memristors through Internal Ionic Dynamics. *Adv. Funct. Mater.* **2015**, *25* (27), 4290-4299.
24. Woodruff, D. N.; Winpenny, R. E. P.; Layfield, R. A., Lanthanide Single-Molecule Magnets. *Chem. Rev.* **2013**, *113* (7), 5110-5148.
25. Feringa, B. L., *Molecular Switches*. Wiley-VCH Verlag GmbH: 2001; p 1-30.
26. Bernot, K.; Bogani, L.; Caneschi, A.; Gatteschi, D.; Sessoli, R., A Family of Rare-Earth-Based Single Chain Magnets: Playing with Anisotropy. *J. Am. Chem. Soc.* **2006**, *128* (24), 7947-7956.
27. Altomare, A.; Burla, M. C.; Camalli, M.; Casciarano, G. L.; Giacovazzo, C.; Guagliardi, A.; Moliterni, A. G. G.; Polidori, G.; Spagna, R., SIR97: A New Tool for Crystal Structure Determination and Refinement. *J. Appl. Crystallogr.* **1999**, *32*, 115-119.
28. Sheldrick, G. M.; Schneider, T. R., SHELXL: High-Resolution Refinement. *Methods Enzymol.* **1997**, *277*, 319-343.
29. Farrugia, L. J., WinGX Suite for Small-Molecule Single-Crystal Crystallography. *J. Appl. Crystallogr.* **1999**, *32*, 837-838.

Captions for Figures

Figure 1. View of compound DyPraNO with labeling scheme. Hydrogen and fluorine atoms are omitted for clarity.

Figure 2. (a) Emission spectra of **Eu-**, **Tb-** and **DyPraNO** (from top to bottom). Evolution of the emission spectra upon addition of Cu^{2+} ions in ethanol solutions of (b) **Eu-**, (c) **Tb-** and (d) **DyPraNO**, respectively. The excitation wavelength is set at 350 nm.

Figure 3. (a) Cross-sectional scanning electron microscopic image and schematic illustration of the ITO/**LnPraNO**/ Cu^{2+} ions@PEO/Pt device. (b) X-ray diffraction pattern of the **EuPraNO** film. (c) Schematic illustration of the migration and distribution of ions upon electric field (the blue spheres stand for the mobile Cu^{2+} ions).

Figure 4. (a) Photoluminescence spectra of the Eu-based device after being subjected to various voltages for 5 s, respectively. (b) Time-dependent luminescence intensity of the device at 615 nm after being subjected to a voltage pulse of -2.5 V for 5 s. (c) Reproducible normalized photoluminescence intensity of the device at 615 nm against alternating negative and positive electric fields (The luminescent intensity is normalized by the initial luminescent intensity of the device at 615 nm).

Figure 5. Photoluminescence spectra of the (a) Tb and (b) Dy-based devices after being subjected to various electric fields. Reproducible normalized photoluminescence intensity of (c) Tb-based device at 545 nm and (d) Dy-based device at 575 nm against alternating negative and positive electric fields (The luminescent intensity is normalized by the initial luminescent intensity of the device at 545 nm and 575 nm, respectively).

Figure 6. Illustration of electrical driven wavelength-dependent information storage based on the different luminescence states of devices made of **EuPraNO**, **TbPraNO** and **DyPraNO**.

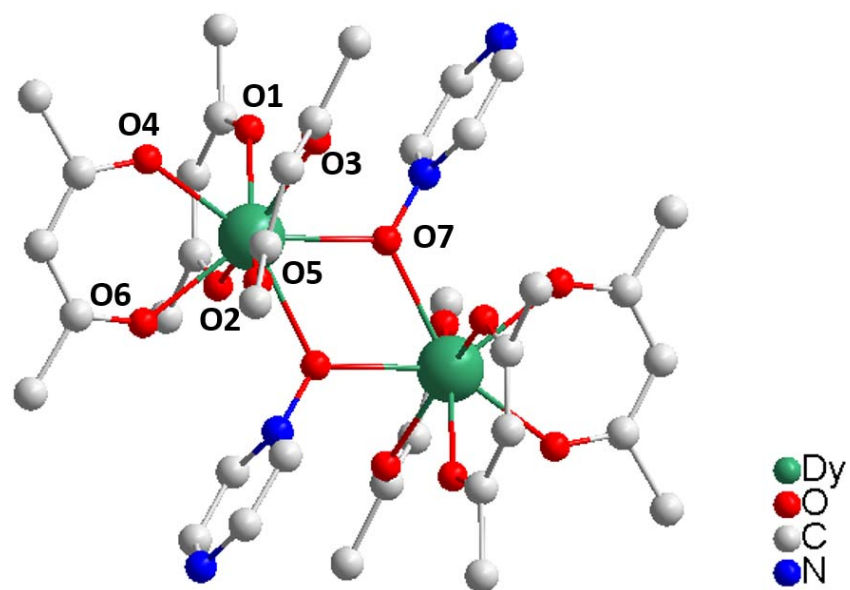


Figure 1. View of compound DyPraNO with labeling scheme. Hydrogen and fluorine atoms are omitted for clarity.

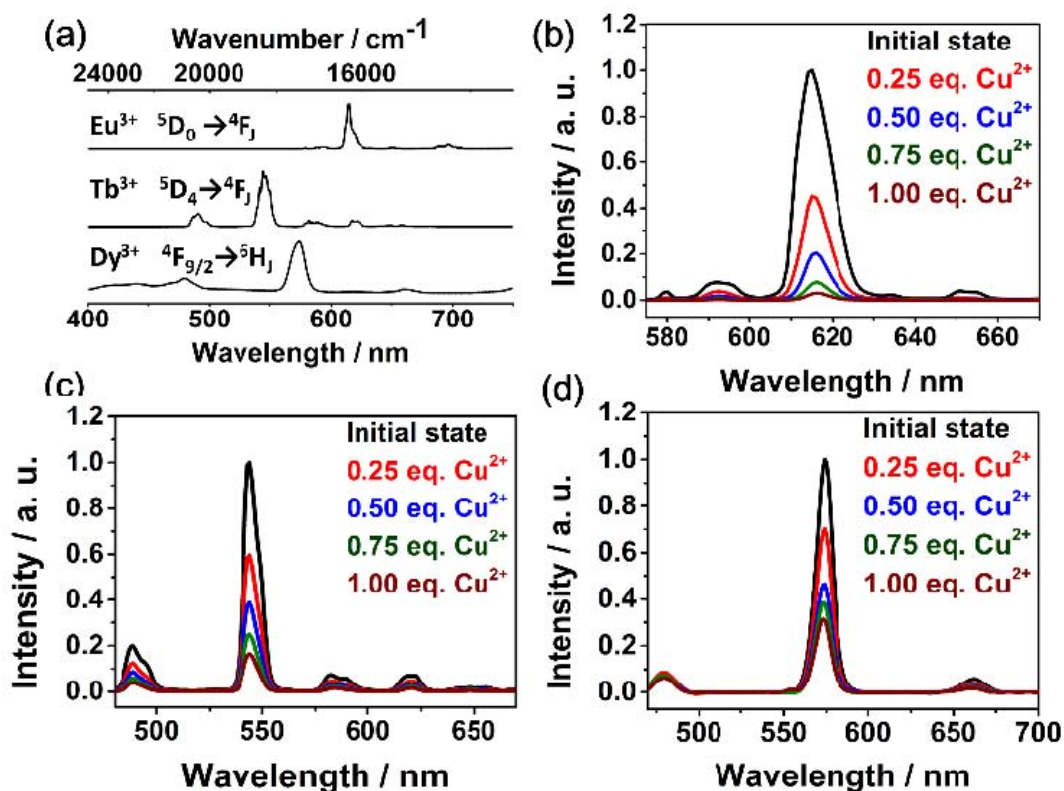


Figure 2. (a) Emission spectra of Eu-, Tb- and DyPraNO (from top to bottom). Evolution of the emission spectra upon addition of Cu²⁺ ions in ethanol solutions of (b) Eu-, (c) Tb- and (d) DyPraNO, respectively. The excitation wavelength is set at 350 nm.

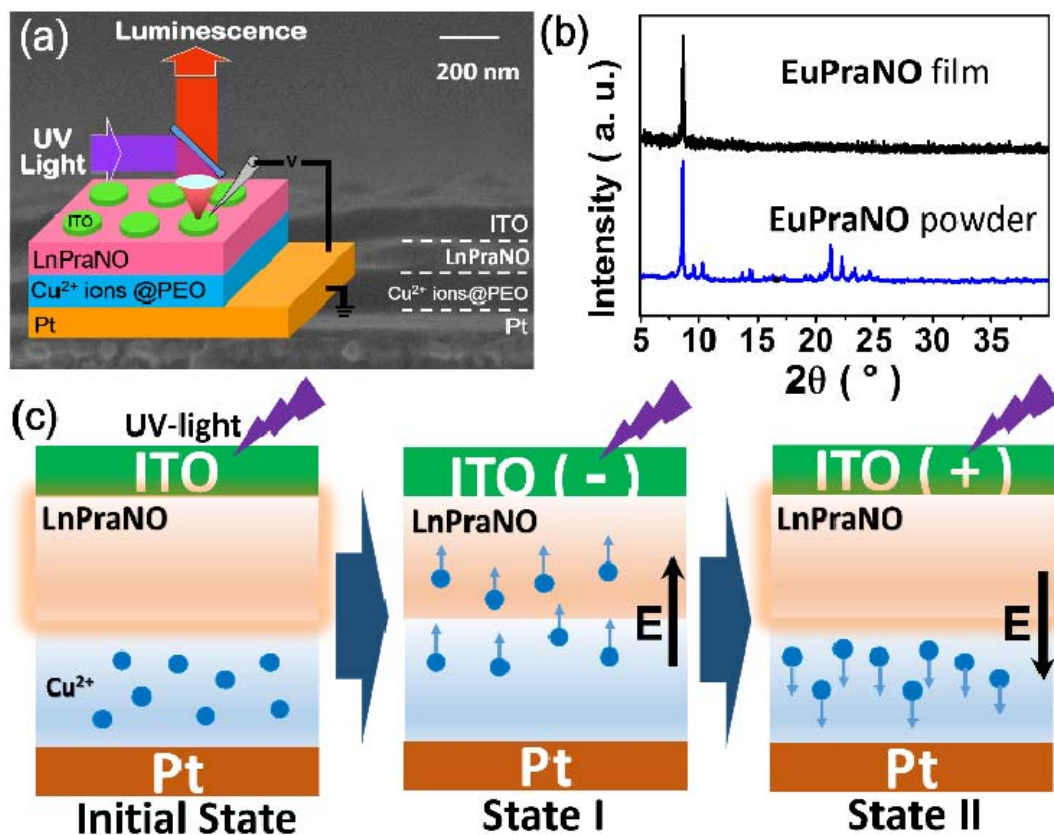


Figure 3. (a) Cross-sectional scanning electron microscopic image and schematic illustration of the ITO/LnPraNO/Cu²⁺ ions@PEO/Pt device. (b) X-ray diffraction pattern of the **EuPraNO** film. (c) Schematic illustration of the migration and distribution of ions upon electric field (the blue spheres stand for the mobile Cu²⁺ ions).

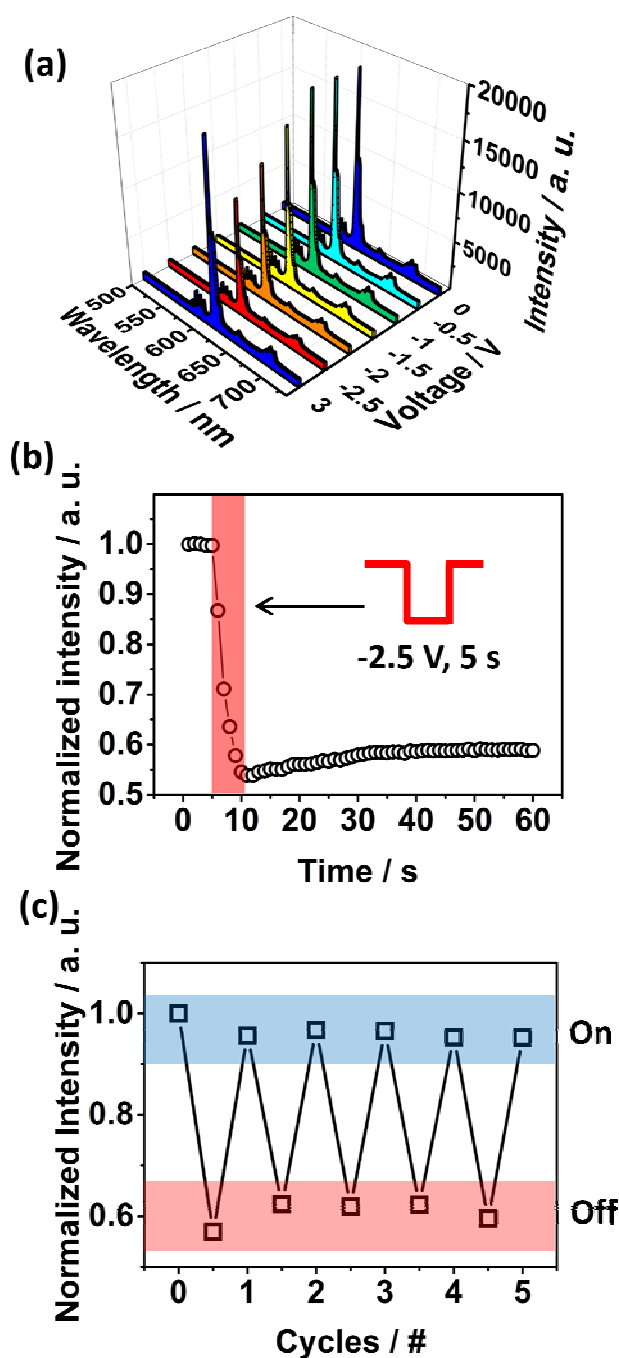


Figure 4. (a) Photoluminescence spectra of the Eu-based device after being subjected to various voltages for 5 s, respectively. (b) Time-dependent luminescence intensity of the device at 615 nm after being subjected to a voltage pulse of -2.5 V for 5 s. (c) Reproducible normalized photoluminescence intensity of the device at 615 nm against alternating negative and positive electric fields (The luminescent intensity is normalized by the initial luminescent intensity of the device at 615 nm).

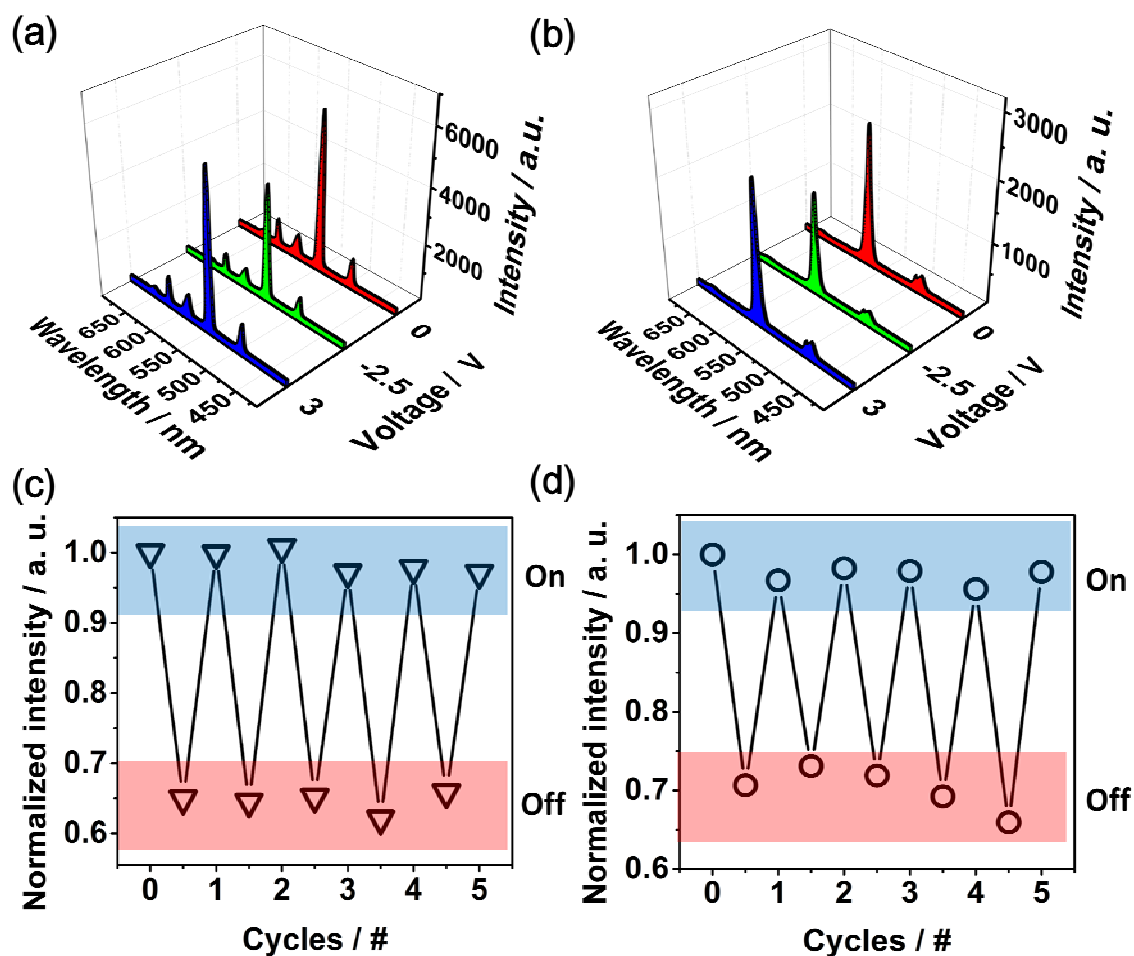


Figure 5. Photoluminescence spectra of the (a) Tb and (b) Dy-based devices after being subjected to various electric fields. Reproducible normalized photoluminescence intensity of (c) Tb-based device at 545 nm and (d) Dy-based device at 575 nm against alternating negative and positive electric fields (The luminescent intensity is normalized by the initial luminescent intensity of the device at 545 nm and 575 nm, respectively).

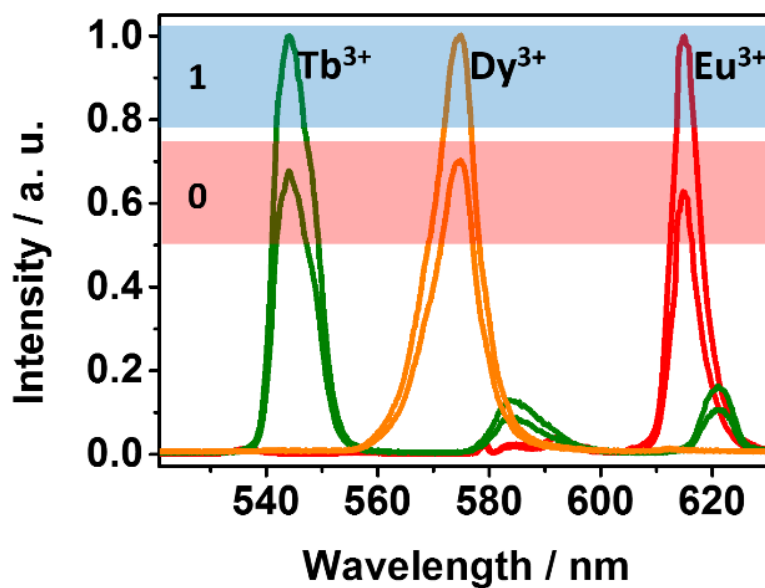
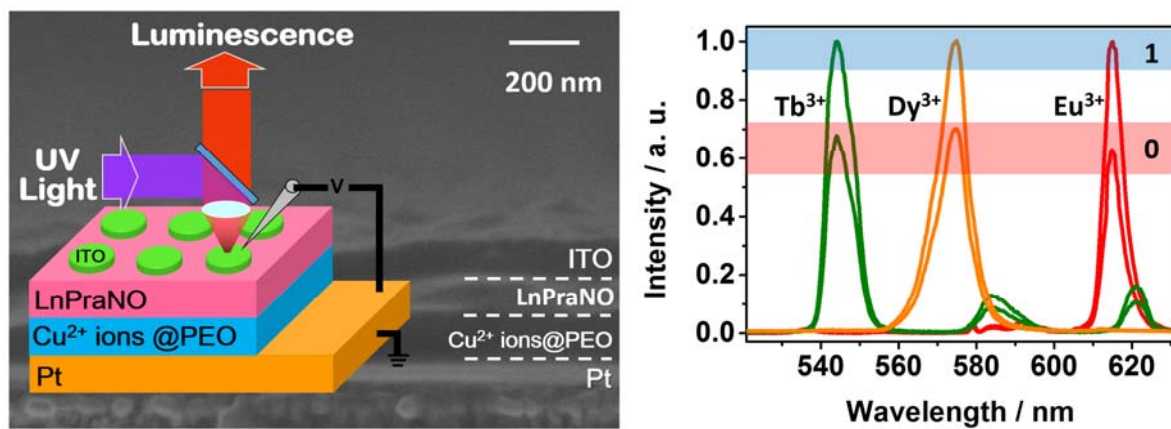


Figure 6. Illustration of electrical driven wavelength-dependent information storage based on the different luminescence states of devices made of **EuPraNO**, **TbPraNO** and **DyPraNO**.

Table of Contents Graphic and Synopsis



Reversible luminescence modulation upon electric field is achieved on a full solid-state device based on lanthanide dimers. Additionally, single-molecule magnets properties of some derivatives offer new hints for multiple level data storage devices.